Hot spots and nonhydraulic effects in surface gravity flows

T. B. Moodie[1], J. P. Pascal[2] & S. J. D. D'Alessio[3]
[1] Applied Mathematics Institute, University of Alberta, Edmonton, Canada
[2] Department of Mathematics, Ryerson University, Toronto, Canada
[3] Department of Applied Mathematics, University of Waterloo, Waterloo, Canada

Abstract

Surface gravity currents whose flow dynamics are modified by incoming solar radiation are of importance in the study of mechanisms related to the thermal bar in dimictic lakes as well as the spread of pollutants on the surfaces of reservoirs, lakes and oceans. We shall present results for such surface flows showing their dependence on various model parameters including the bottom slope, rate of heating and equation of state. The novel feature of this analysis is to show that the inclusion of a heat source term leads to the introduction of shear in the horizontal velocity field thereby ruling out the deployment of shallow-water theory with its depth-independent velocity field as a viable description of such flows. Calculations are presented to demonstrate that a purely hydraulic description will miss important dynamical features of the flows.
Keywords: surface gravity currents, thermal enhancement, nonhydraulic effects.

1 Introduction

A gravity current consists of the flow of one fluid within another when this flow is driven by the density difference between these fluids [1]. These currents are primarily horizontal, occurring as either top or bottom boundary currents or as intrusions at some buoyantly stable intermediate level. The density differences driving such flows may be due to salinity contrasts, as in oceanic settings [1], the presence of suspended material, as in the case of turbidity currents [2, 3], or temperature

WIT Transactions on Engineering Sciences, Vol 52, © 2006 WIT Press
www.witpress.com, ISSN 1743-3533 (on-line)
doi:10.2495/AFM06018

contrasts [4–6], as in the case to be treated here, or combinations of these mechanisms.

In the gravity current literature researchers have employed, in general, two different approaches. One direction of research has used hydraulic theory to study the time evolution of these currents from a state of rest while the other investigates the steady-state characteristics of a gravity current that has already been established without any concern for initial conditions [7]. It is, we believe, fair to say that this latter approach, which treats the current as steady, requires pressure balances that essentially rule out the inclusion of most of those physical processes that make these investigations important from the point of view of applications. Such processes would include the entrainment and sedimentation of particles that drive turbidity currents [8], the spatial and temporal influences of heating that modify the dynamics through density changes [5, 6] as well as the various flow modifications that arise from topographic forcing [9]. Adopting the former approach is not without difficulties when it comes to including these processes in the model formulation but it does offer an avenue of approach that the latter does not afford.

Our previous studies [3, 10, 11] have indicated that in the modelling of turbidity currents with sedimenting particles, horizontal gradients in particle concentrations result in a depth-dependent horizontal velocity field.

This depth dependence signifies that the deployment of shallow-water theory for these low aspect ratio flows must be brought into question. In the present analysis of thermally-enhanced surface gravity flows we will show that there is an analogous mechanism at work leading to ‘hot spots’ in the flow field that ultimately rules out the use of the standard shallow-water model for such flows.

In this article we develop and analyze a two layer fluid model governing the sudden release and subsequent motion of a fixed volume of light fluid whose initial density and temperature are ρ_* and T_*, respectively.These fixed volume releases have served as a paradigm for many atmospheric [12] and oceanic [1] gravity currents although it is the case that many of these flows being modelled arise not from a fixed volume release but rather from variable inflow through an opening in some barrier[13, 14]. We will provide some suggestions as to how such variable inflow problems might be approached but for now we consider our fixed volume as being released suddenly into a heavier ambient fluid of constant density $\rho_0 > \rho_*$ overlying a gently sloping bottom. The upper layer is subjected to incoming radiation and its density is assumed to decrease in time according to a general equation of state. The surface heat flux is assumed to be distributed uniformly over the local thickness of the upper layer [15]. This upper layer thickness being a function of both space and time will lead to a temperature field which is also a function of space and time with an increased heating rate for patches where upper layer thickness is diminished due to the unsteady nature of the flow. These radiation induced horizontal temperature gradients introduce distinctive $O(1)$ nonhydraulic effects into the flow field. This dependence of heating rate on the local depth of the heated fluid layer is consistent with observations in lakes and reservoir sidearms subjected to diurnal heating and cooling [15–17]. A similar mechanism is seen in bottom-hugging turbidity currents when sedimentation rate depends on the thickness of the current [10]. In that instance sedimentation rates are greater for regions where the current is thinner leading to local decreases in the bulk density and hence the generation of horizontal gradients in the density field. It is these horizontal density gradients for both turbidity and thermally enhanced gravity currents that lead to the nonhydraulic nature of these flows.

2 Model formulation

We consider a gravity current produced by the release of a fixed volume of fluid having initial density $\rho_1 = \rho_*$ into an ambient fluid having a higher density $\rho_2 = \rho_0$(constant) overlying a mildly sloping bottom. The physical configuration is depicted in Figure 1, where $\eta(x,t)$ represents the displacement of the free surface from its undisturbed configuration, $\mathbf{u} = (u, w)$ is the fluid velocity in Cartesian coordinates with position vector $\mathbf{x} = (x, z)$, H is the mean depth of the two layer system measured from $z = 0$, $h(x,t)$ is the variable thickness of the lighter upper fluid layer and the bottom is located at $z = -sf(x)$, where $s(0 < s \ll 1)$ is a nondimensional slope parameter. In this study we will only consider a linearly varying bottom and thus set $f(x) = x$. The flow is driven by the buoyancy force arising because of the difference between the temperature dependent density $\rho_1(T)$ of the upper layer and the fixed density $\rho_2 = \rho_0$ of the ambient fluid. The relation between temperature and density for the upper layer is given in terms of an equation of state which will be assumed to have the general form

$$\rho_1(T) = \rho_0 \left[1 - \alpha(T - T_0)^n\right], \quad n = 1, 2, \tag{1}$$

wherein T_0 is the fixed temperature of the lower layer whose density is assumed fixed at ρ_0, α is the thermal expansion coefficient, and $n > 0$ is a power law index. Since the temperature of the lower layer is assumed to remain fixed we have chosen to measure the temperature $T_1 \equiv T$ of the upper layer relative to this fixed value. We shall take $T = T_* > T_0$ as the initial temperature of the release volume so that

$$\rho_1(T_*) = \rho_* = \rho_0 \left[1 - \alpha(T_* - T_0)^n\right] < \rho_0. \tag{2}$$

We have chosen to take $n = 1, 2$ in our study since these are natural choices. The case $n = 1$ corresponds to the usual description whereby the density decreases linearly with an increase in temperature. The case $n = 2$ can be used to approximate the density of fresh water near the temperature of maximum density [17], that is, $T_0 \approx 4\,^\circ\mathrm{C}$. Here with $n = 2$ we would have $\alpha = 1.65 \times 10^{-5}\,^\circ\mathrm{C}^{-2}$.

Shown in Figure 1 is the released fixed volume of fluid which initially occupied the region $0 < z \leq H$. Assuming small temperature differences the Boussinesq approximation for the density is appropriate and will be invoked throughout our model development. We shall assume a surface heat flux I which is distributed uniformly over the local depth of the upper layer with no heating of the denser

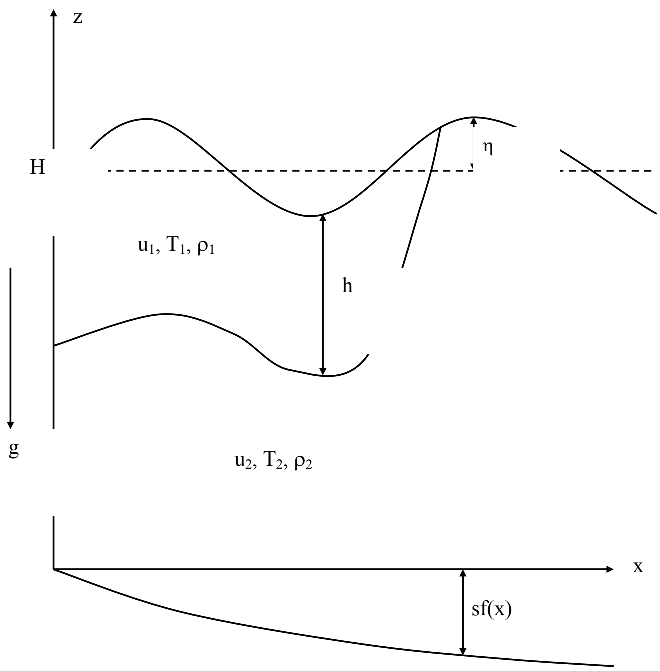

Figure 1: The flow configuration of the two layer fluid model.

ambient fluid. This leads to a heat source term in the temperature equation of the form

$$Q = \frac{I}{\rho_0 C_p h_0} \,{}^\circ\mathrm{C\,s}^{-1}. \tag{3}$$

In the above h_0 denotes a representative depth over which the heat flux I has been distributed, ρ_0 is the reference density and C_p is the specific heat at constant pressure. The magnitude of Q increases as h_0 decreases and this will give rise to horizontal gradients in temperature and hence also in the temperature dependent density which will augment the driving buoyancy forces in the flow as well as induce $O(1)$ nonhydraulic effects into the upper layer flow field. These horizontal gradients arising because of the x-dependence in the heat source term were noted by Farrow [4] in his study of the hydrodynamics of the thermal bar. Our inclusion of the variable thickness of the upper layer in the heat source term for a fully transient two layer model has, to the best of our knowledge, not been attempted in the literature to date.

In all of our development we will assume that the Reynolds numbers, Re, of the flow are sufficiently large that viscous forces are negligible and that the flow dynamics are dominated by a balance between buoyancy and inertial forces. As for the viscous effects resulting from the boundary layer formed adjacent to the bottom solid boundary, we deem these to be insignificant because the thickness of this layer, which is $O(L/\sqrt{Re})$ with L denoting the horizontal length scale associated with the motion, remains well away from the interface of our two layer model. Hence viscous effects from the bottom are not communicated to the top layer. Further, the approximation made in ignoring the bottom boundary layer is consistent with the small aspect ratio assumption made in this work. We have taken the sole conservative body force to be that of gravity and neglected the effects of surface tension at the interface. This latter assumption requires that the Bond number $B = \rho g' L^2/\sigma \gg 1$, where g' is the reduced gravity and σ the surface tension [18]. We have further assumed that the flows are sufficiently rapid and small scale that the effect of the earth's rotation can be neglected. This requires that the Rossby number $R_0 = U/fL \gg 1$, where f is the Coriolis parameter and U and L are characteristic velocity and length scales of the flow [18]. The non-rotating case considered here is relevant to laboratory scale flows and has been employed in studies of the thermal bar [4, 15].

We now adapt the equations of mass and momentum balance to study low aspect ratio flows involving two active coupled layers consisting of an absorbing upper layer having a temperature dependent density overlying a homogeneous fluid of fixed density that is in contact with a gently sloping impermeable bottom. Our choice of non-dimensional and scaled variables are given according to the following scheme:

$$x = L\widetilde{x},\, z = h_0\widetilde{z},\ t = \frac{L}{U}\widetilde{t},\ h = h_0\widetilde{h},\ H = h_0\widetilde{H},\ (u_1,u_2) = U(\widetilde{u}_1,\widetilde{u}_2),$$
$$(w_1,w_2) = \frac{h_0U}{L}(\widetilde{w}_1,\widetilde{w}_2),\ (p_1,p_2) = U^2\rho_0(\widetilde{p}_1,\widetilde{p}_2),\ \eta = \frac{U^2}{g}\widetilde{\eta}, \quad (4)$$
$$s = \delta\widetilde{s},\ \theta = T - T_0 = \theta_0\widetilde{\theta},\ U^2 = g'h_0,\ \delta = \frac{h_0}{L},$$

where we have chosen the temperature scale $\theta_0 = T_* - T_0$ to be the initial temperature difference between the two layers and the reduced gravity g' to be defined in terms of the initial density contrast, that is

$$g' = \frac{\rho_0 - \rho_*}{\rho_0}g = \alpha\theta_0^n g. \quad (5)$$

The aspect ratio $\delta = h_0/L$ is assumed small, that is, $0 < \delta \ll 1$.We have chosen the advective time scaling L/U for our model in order to be consistent with our assumption that there is no heat transfer between the fluid layers. This assumption requires that the diffusive or convective time scale given by $t_d \sim h_0^2/\kappa$, where κ is the thermal diffusivity, be much larger than the advective time scale.

In the nondimensional equations to follow, (6)–(9) provide for horizontal and vertical momentum balances in the two layers whereas (10)–(14) give the dynamic and kinematic boundary conditions at the free surface, interface and bottom boundary with tildes dropped from nondimensional quantities:

$$\frac{\partial u_1}{\partial t} + u_1\frac{\partial u_1}{\partial x} + w_1\frac{\partial u_1}{\partial z} = -\frac{\partial p_1^*}{\partial x}, \quad (6)$$

$$\delta^2\left(\frac{\partial w_1}{\partial t}+u_1\frac{\partial w_1}{\partial x}+w_1\frac{\partial w_1}{\partial z}\right)=-\frac{\partial p_1^*}{\partial z}+\theta^n, \tag{7}$$

$$\frac{\partial u_2}{\partial t}+u_2\frac{\partial u_2}{\partial x}+w_2\frac{\partial u_2}{\partial z}=-\frac{\partial p_2^*}{\partial x}, \tag{8}$$

$$\delta^2\left(\frac{\partial w_2}{\partial t}+u_2\frac{\partial w_2}{\partial x}+w_2\frac{\partial w_2}{\partial z}\right)=-\frac{\partial p_2^*}{\partial z}, \tag{9}$$

$$\alpha\theta_0^n p_1^*\left(x,H+\alpha\theta_0^n\eta,t\right)=H+\alpha\theta_0^n\eta \tag{10}$$

$$w_1\left(x,H+\alpha\theta_0^n\eta,t\right)=\alpha\theta_0^n\left(\frac{\partial\eta}{\partial t}+u_1\left(x,H+\alpha\theta_0^n\eta,t\right)\frac{\partial\eta}{\partial x}\right), \tag{11}$$

$$p_1^*\left(x,H+\alpha\theta_0^n\eta-h,t\right)=p_2^*\left(x,H+\alpha\theta_0^n\eta-h,t\right), \tag{12}$$

$$w_i\left(x,H+\alpha\theta_0^n\eta-h,t\right)=\alpha\theta_0^n\left(\frac{\partial\eta}{\partial t}+u_i\left(x,H+\alpha\theta_0^n\eta-h,t\right)\frac{\partial\eta}{\partial x}\right)$$
$$-\left(\frac{\partial h}{\partial t}+u_i\left(x,H+\alpha\theta_0^n\eta-h,t\right)\frac{\partial h}{\partial x}\right),\quad i=1,2, \tag{13}$$

$$w_2\left(x,-sx,t\right)=-su_2\left(x,-sx,t\right). \tag{14}$$

In the above p_i^* refers to the dynamic pressure fields in the two fluids.

Under the assumption $0<\delta^2\ll 1$ we see that the horizontal velocity field in the lower layer is independent of z whereas that in the upper layer retains its z-dependence. Integrating the mass balance equation for the lower layer over the depth and applying the kinematic boundary conditions gives the mass balance to be

$$\frac{\partial}{\partial t}\left(h-\alpha\theta_0^n\eta\right)+\frac{\partial}{\partial x}\left[\left(h-\alpha\theta_0^n\eta-H-sx\right)u_2\right]=0. \tag{15}$$

Pressure continuity at the interface provides $p_2^*=\eta-\theta^n h+H(\alpha\theta_0^n)^{-1}$ leading directly to the horizontal momentum equation for the lower layer as

$$\frac{\partial u_2}{\partial t}+\frac{\partial}{\partial x}\left(\frac{1}{2}u_2^2+\eta-\theta^n h\right)=0. \tag{16}$$

Since it is straightforward to show that $\partial p_1^*/\partial x$ is a function of z it follows that $u_1=u_1\left(x,z,t\right)$. Integrating the mass balance equation for the upper layer and applying the kinematic boundary conditions gives for continuity in that layer

$$\frac{\partial h}{\partial t}+\frac{\partial}{\partial x}\left(\int_{H+\alpha\theta_0^n\eta-h}^{H+\alpha\theta_0^n\eta}u_1(x,z,t)dz\right)=0. \tag{17}$$

It now remains for us to specify the heat equation to complete the model. With the surface heat flux I assumed to be distributed uniformly over the local thickness

$h(x,t)$ of the upper layer and applying conservation principles we have that

$$\frac{\partial}{\partial t}(h\theta) + \frac{\partial}{\partial x}\left(\theta \int_{H+\alpha\theta_0^n\eta-h}^{H+\alpha\theta_0^n\eta} u_1(x,z,t)\,dz\right) = Q, \qquad (18)$$

where

$$Q = \frac{I}{\rho_0 C_p h_0} {}^\circ C s^{-1}, \qquad Q = \frac{U\theta_0}{L}\widetilde{Q}. \qquad (19)$$

Employing (17) in (18) we can then express the heat equation as

$$\frac{\partial\theta}{\partial t} + \frac{1}{h(x,t)}\left(\int_{H+\alpha\theta_0^n\eta-h}^{H+\alpha\theta_0^n\eta} u_1(x,z,t)dz\right)\frac{\partial\theta}{\partial x} - \frac{Q}{h(x,t)} = 0. \qquad (20)$$

Our model equations now consist of the lower layer mass balance and momentum equations (15) and (16), upper layer momentum and mass balance equations (6) and (17), respectively and the heat equation (20).

3 Some numerical results

All of our numerical results obtained for fixed volume releases involved first expanding $u_1(x,z,t)$ in the form of a power series about the variable position of the upper layer's lower boundary $z_0 = H + \alpha\theta_0^n\eta - h$. Substituting into the model equations and truncating the series leads to a system of eight equations in eight unknowns which can be written in vector form as

$$\frac{\partial \mathbf{U}}{\partial t} + \frac{\partial \mathbf{F}}{\partial x} = \mathbf{B}, \qquad (21)$$

where $\mathbf{U}$ is a vector consisting of the flow variables, $\mathbf{F}$ is the corresponding flux vector and $\mathbf{B}$ refers to any source terms present in our system. We applied MacCormack's method [19] together with a strategy proposed by Lapidus [20] for damping spurious oscillations. Some results are displayed in Figures 2 and 3.

In Figure 2 we have plotted the evolution of the thickness of the gravity current for the hydraulic and nonhydraulic cases. The hydraulic model corresponds to the case wherein the temperature field is independent of the horizontal coordinate. This is in contrast to the model developed here wherein heating rates depend on the local thickness $h(x,t)$ of the heated layer resulting in a spatially dependent temperature field. It is clear that the gravity current speed is greater for the nonhydraulic case which will, in turn, lead to an increased rate of thinning of the current and a higher heating rate with increased buoyancy forces arising as a result of the increased density contrast between the two layers.

In Figure 3 we have plotted the total pressure field along the interface given by $z = H + \alpha\theta_0\eta - h$ for the hydraulic and nonhydraulic cases. We see that the total pressure field for the nonhydraulic case falls off more rapidly than does that associated with the hydraulic model. This is a result of the increased rate of

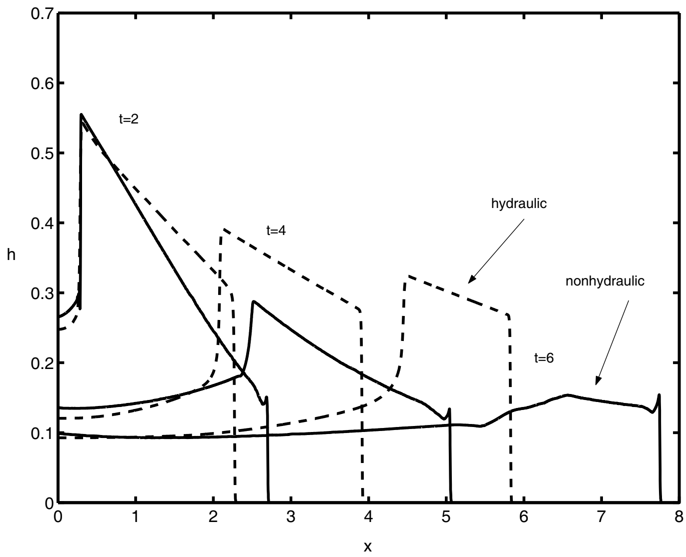

Figure 2: The evolution of the thickness of the gravity current with $n = 1, Q = 0.5, g'/g = 0.05, h_* = 0.9$.

thinning of the current in the nonhydraulic case coupled with increased heating rates. The relatively level profile for the pressure that is achieved around elapsed times $t \approx 6$ in the nonhydraulic case corresponds to the similarly level profile for the thickness of the current that is displayed in Figure 2 for the same parameter values. It is clear that there are substantial differences between the pressures for these two cases.

4 Some closing remarks

In contrast to the large amount of published theoretical and experimental material on gravity currents arising from fixed volume releases, that for variable inflow gravity currents is relatively small. This is in spite of the fact that when many gravity currents are initiated by, say, an accidental release of a fluid into an ambient environment, there is a variable discharge of fluid through an opening in a barrier. This would be the case in the situation when the rupture of a storage tank or pipeline gives rise to the release of a fluid at a variable rate over a period of time. Variable inflow gravity currents are also of great interest to those involved in the study of fluid motions in the natural environment that are not the result of contaminant releases. For example, flows of fresh water from spring run-off into lakes and fjords rarely take place with a constant flow rate, and the consequent evolution of the intrusions thus formed may be incorrectly estimated by using a constant flow model. A number of similar scenarios with flash floods, flows from volcanoes,

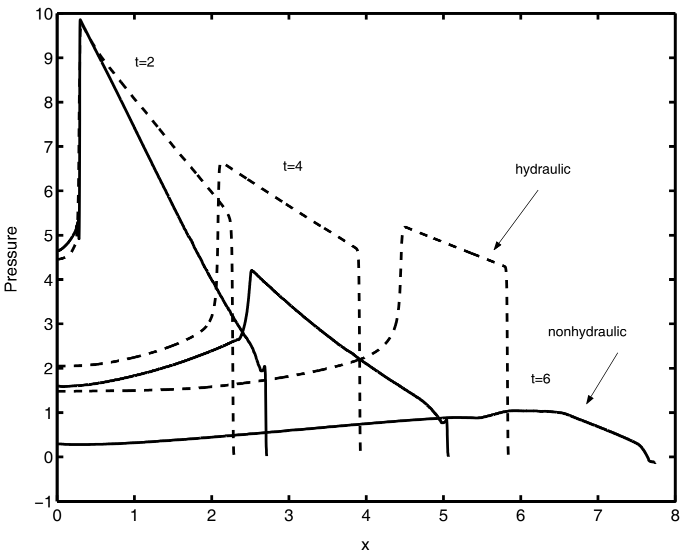

Figure 3: The evolution of the pressure at the interface between the two fluids with $n = 1, Q = 0.5, g'/g = 0.05, h_* = 0.9$.

discharges from locks in canals connecting lakes etc., all involve variable inflow buoyancy driven flows.

To develop a model for several of the above scenarios relating to variable inflow gravity currents one could consider a large volume of inviscid and incompressible fluid having a fixed temperature T_* and density ρ_* initially at rest behind a lock gate in which a small opening of height $h_0 \ll H$ is suddenly formed while a variable pressure is applied to the surface of this fluid. This mimics the conditions pertaining to the sudden rupture of an onshore storage container that then debouches its contents into a large body of water at a variable rate to create a variable inflow surface gravity current. Using energy principles and continuity it is possible to show that the average velocity through the narrow opening, $\overline{u}_1$, is governed by the forced Riccati equation

$$\frac{d\overline{u}_1}{dt} + \frac{L^2}{\overline{s}h_0}\frac{\overline{u}_1^2}{2} = \frac{L^2}{\overline{s}h_0}p(t) + \frac{L^2}{2\overline{s}h_0}, \quad \overline{u}_1(0) = 0,$$

where L is the horizontal dimension of the container and $\overline{s}$ the average length of a streamline extending from a point on the surface of the fluid in the lock to a point in the narrow orifice. Solving this initial value problem then gives a reasonable value for the variable inflow velocity.

References

[1] J.E.Simpson, *Gravity Currents: In the Environment and the Laboratory, 2nd ed.,* Cambridge University Press, Cambridge, England, 1997.

[2] R.T.Bonnecaze, H.E.Huppert, J.R.Lister, Particle-driven gravity currents, *J.Fluid Mech.,* **250**, pp.339-369, 1993.

[3] T.B.Moodie, J.P.Pascal, Non-hydraulic effects in particle-driven gravity currents in deep surroundings, *Stud.Appl.Math.,* **107**, pp.217-251, 2001.

[4] D.E.Farrow, An asymptotic model for the hydrodynamics of the thermal bar, *J.Fluid Mech.,* **289**, pp.129-140, 1995.

[5] S.J.D.D'Alessio, J.P.Pascal, T.B.Moodie, Thermally enhanced gravity driven flows, *J.Comp.Appl.Math.,* **170**, pp.1-25, 2004.

[6] T.B.Moodie, J.P.Pascal, S.J.D.D'Alessio, Non-hydraulic effects in two- layer thermally-enhanced gravity-driven flows, *Int.J.Nonlinear Mech.,* **40,** pp.11-25, 2005.

[7] T.B.Benjamin, Gravity currents and related phenomena, *J.Fluid Mech.,* **31**, pp.209-248, 1968.

[8] D.Pritchard, A.J.Hogg, On sediment transport under dam-break flow, *J.Fluid Mech.,* **473**, pp.265-274, 2002.

[9] D.Z.Zhu, G.A.Lawrence, Non-hydrostatic effects in layered shallow water flows, *J.Fluid Mech.,* **355**, pp.1-16, 1998.

[10] T.B.Moodie, J.P.Pascal, G.E.Swaters, Sediment transport and deposition from a two-layer fluid model of gravity currents on sloping bottoms, *Stud.Appl.Math.,* **100**, pp.215-244, 1998.

[11] T.B.Moodie, J.P.Pascal, J.C.Bowman, Modeling sediment deposition patterns arising from suddenly released fixed-volume turbulent suspensions, *Stud.Appl.Math.,* **105**, pp.333-359, 2000.

[12] J.B.Klemp, R.Rotunno, W.C.Skamarock, On the dynamics of gravity currents in a channel, *J.Fluid Mech.,* **269**, pp.169-198, 1994.

[13] T.Maxworthy, Gravity currents with variable inflow, *J.Fluid Mech.,* **128**, pp.247-257, 1983.

[14] J.Gratton, C.Vigo, Self-similar gravity currents with variable inflow revisited: plane currents, *J.Fluid Mech.,* **258**, pp.77-104, 1994.

[15] D.E.Farrow, J.C.Patterson, On the response of a reservoir sidearm to diurnal heating and cooling, *J.Fluid Mech.,* **246**, pp.143-161, 1993.

[16] S.Zilitinkevich, K.D.Kreiman, A.Y.Terzhevik, The thermal bar, *J.Fluid Mech.,* **236**, pp.27-42, 1992.

[17] J.Malm, S.Zilitinkevich, Temperature distribution and current system in a convectively mixed lake, *Bound. Layer Meteor.,* **71**, pp.219-234, 1994.

[18] J.Pedlosky, *Geophysical Fluid Dynamics,* 2nd Ed., Springer, New York, 1986.

[19] R.LeVeque, *Numerical Methods for Conservation Laws*, Birkhäuser, Basel, 1992.

[20] A.Lapidus, A detached shock calculation by second-order finite differences, *J.Comp.Phys.,* **2**, pp.154-177, 1967.